Radixin, a Barbed End-capping Actin-modulating Protein, Is Concentrated at the Cleavage Furrow during Cytokinesis

Naruki Sato,*‡ Shigenobu Yonemura,* Takashi Obinata,‡ Sachiko Tsukita,* and Shoichiro Tsukita*

*Department of Information Physiology, National Institute for Physiological Sciences, Myodaiji, Aichi 444; and ‡Department of Biology, Chiba University, Yayoi-cho, Chiba 260, Japan

Abstract. Radixin is a barbed end-capping actin-modulating protein which was first identified in isolated cell-to-cell adherens junctions from rat liver (Tsukita, Sa., Y. Hieda, and Sh. Tsukita, 1989. *J. Cell Biol.* 108:2369–2382). In the present study, we have analyzed the distribution of radixin in dividing cells. For this purpose, an mAb specific for radixin was obtained using chicken gizzard radixin as an antigen. By immunofluorescence microscopy with this mAb and a polyclonal antibody obtained previously, it was clearly shown in rat fibroblastic cells (3Y1 cells) that radixin was highly concentrated at the cleavage furrow during cytokinesis. Radixin appeared to accumulate rapidly at the cleavage furrow at the onset of furrowing, continued to be concentrated at the furrow during anaphase and telophase, and was finally enriched at the midbody. This concentration of radixin at the cleavage furrow was detected in all other cultured cells we examined: bovine epithelial cells (MDBK cells), mouse myeloma cells (P3 cells), rat kangaroo Ptk2 cells, mouse teratocarcinoma cells, and chicken fibroblasts. Furthermore, it became clear that the epitope for the mAb was immunofluorescently masked in the cell-to-cell adherens junctions. Together, these results lead us to conclude that radixin is present in the undercoat of the cell-to-cell adherens junctions and that of the cleavage furrow, although their respective molecular architectures are distinct. The possible roles of radixin at the cleavage furrow are discussed with special reference to the molecular mechanism of the actin filament–plasma membrane interaction at the furrow.

ACTIN filaments are involved in many kinds of cell motility and are found in association with the plasma membrane in a variety of eukaryotic cells (18, 28). An obvious function of the association of actin filaments with membranes may be that membranes serve as attachment sites for actin filaments in cell motility systems. In interphase eukaryotic nonmuscle cells, two types of well-developed actin filament bundles which can contract by themselves in cooperation with myosin molecules can be observed: stress fibers in cultured cells and circumferential bundles in epithelial cells (4, 31, 44). They are associated with plasma membranes at the cell-to-substrate and cell-to-cell adherens junctions (AJ),[1] respectively (9, 13, 16, 37). To clarify the molecular organization of these actin filament attachment sites, intensive studies have been made mainly using immunohistochemical methods. So far many proteins have been identified as constituents of the undercoat of AJ. These AJ undercoat-constitutive proteins can be categorized into two groups: group A proteins such as α-actinin (21) and filamin (14), which are localized not only at the AJ undercoat but also along the actin bundles, and group B proteins such as vinculin (12, 15) and talin (2, 3), which are mainly localized at the AJ undercoat.

The other example of the contractile actin bundle is the so-called contractile ring which is formed just beneath the cleavage furrow during cytokinesis (27, 33–35). The molecular organization and mode of membrane association of this type of actin bundle has also continued to attract many investigators, and mainly by immunohistochemical analyses many actin filament-related proteins were checked to see whether they were localized at the cleavage furrow (for reviews see references 22, 29, 36). In particular, to understand the molecular mechanism of the association between actin filaments and plasma membranes at the cleavage furrow, the possible presence of the AJ undercoat-constitutive proteins in the furrow was intensively studied. As a result, many "group A" proteins (α-actinin, filamin, et cetera) were shown to be localized at the cleavage furrow (1, 11, 22, 23, 29, 32, 36), although a recent study has revealed that these proteins show a variable degree of concentration at the furrow (25). In sharp contrast to these proteins, no "group B" protein has been reported to be present at the furrow.

Recently, we have succeeded in isolating the cell-to-cell AJ from rat liver and in identifying 10 major protein constit-

1. *Abbreviations used in this paper*: AJ, adherens junction; HAT, hypoxanthine/aminopterine/thymidine; MDBK, Madin-Darby bovine kidney; pAb, polyclonal antibody; mAb, monoclonal antibody.

uents of its undercoat (40). Through our recent analyses of these proteins, it became clear that some of them belong to group A and some to group B; tenuin (400 kD) is localized both at the AJ undercoat and along the actin bundles (group A) (39), whereas radixin (82 kD) and a 70-kD protein are localized exclusively at the AJ undercoat (group B) (38, 41). Recently, using antibodies specific for these newly identified AJ undercoat-constitutive proteins, we have checked to see whether these proteins occur in the cleavage furrow. In this study, we present data showing that radixin is highly concentrated at the cleavage furrow during cytokinesis in various types of cells. Radixin is a barbed end-capping actin-modulating protein, which belongs to group B as an AJ undercoat-constitutive protein (38). Since this is the first instance of an AJ-undercoat-constitutive protein of group B, which is concentrated at the cleavage furrow, we believe this study will give us a clue for a better understanding of the molecular basis of the actin filament-plasma membrane interaction.

Materials and Methods

Isolation of Cell-to-Cell Adherens Junctions from Rat Liver

The adherens junction was prepared from rat liver by a combination of homogenization, sucrose density gradient centrifugation, and NP-40 treatment as described (40). A low-salt extract containing the undercoat-constitutive proteins was obtained by dialysis of the adherens junction fraction against the extraction solution (1 mM EGTA, 0.5 mM PMSF, 1 g/ml leupeptin, 2 mM Tris-HCl [pH 9.2]), followed by centrifugation at 100,000 *g* for 60 min.

Purification of Rat Radixin and Production of Polyclonal Antibody (pAb) Specific for Radixin

Rat radixin was purified from the low-salt extract of the isolated adherens junctions according to the method developed previously (38). Antisera to this radixin (purified by SDS-PAGE) were elicited in rabbits, and IgG was purified from the sera as described (38).

Purification of Chicken Radixin

The "crude extract" was obtained from chicken gizzard essentially according to the method developed by Feramisco and Burridge (10). Fresh chicken gizzard smooth muscle was dissected and the connective tissue was carefully removed. After being minced with a razor blade, the muscle was blended in 7 vol of distilled water containing 1 mM PMSF and 1 μg/ml leupeptin at 12,000 rpm in a Waring blender three times for 30 s each at 4°C. The homogenate was centrifuged for 10 min at 10,000 rpm, and the pellet was resuspended in 7 vol of distilled water containing 1 mM PMSF and 1 μg/ml leupeptin followed by centrifugation for 10 min at 10,000 rpm at 4°C. The pellet was resuspended in 7 vol of solution A (2 mM Tris, 1 mM EGTA, 0.5 mM PMSF, and 1 μg/ml leupeptin [pH 9.0]) and stirred slowly for 30 min at 30°C. The sample was centrifuged for 10 min at 12,000 rpm at 4°C. The supernatant was adjusted to pH 7.0 with hydrochloric acid followed by addition of 1/100 vol of 1.3 M $MgCl_2$. The suspension was stirred at room temperature for 15 min, and then the crude extract was obtained by centrifugation for 1 hr at 25,000 rpm at 4°C as a supernatant.

Preswollen DEAE-cellulose (DE52; Whatman Instruments Co., Clifton, NJ) was packed into a column (1.5 × 5 cm) and equilibrated with solution B (10 mM Hepes, 1 mM EGTA, 0.5 mM PMSF, 1 μg/ml leupeptin, and

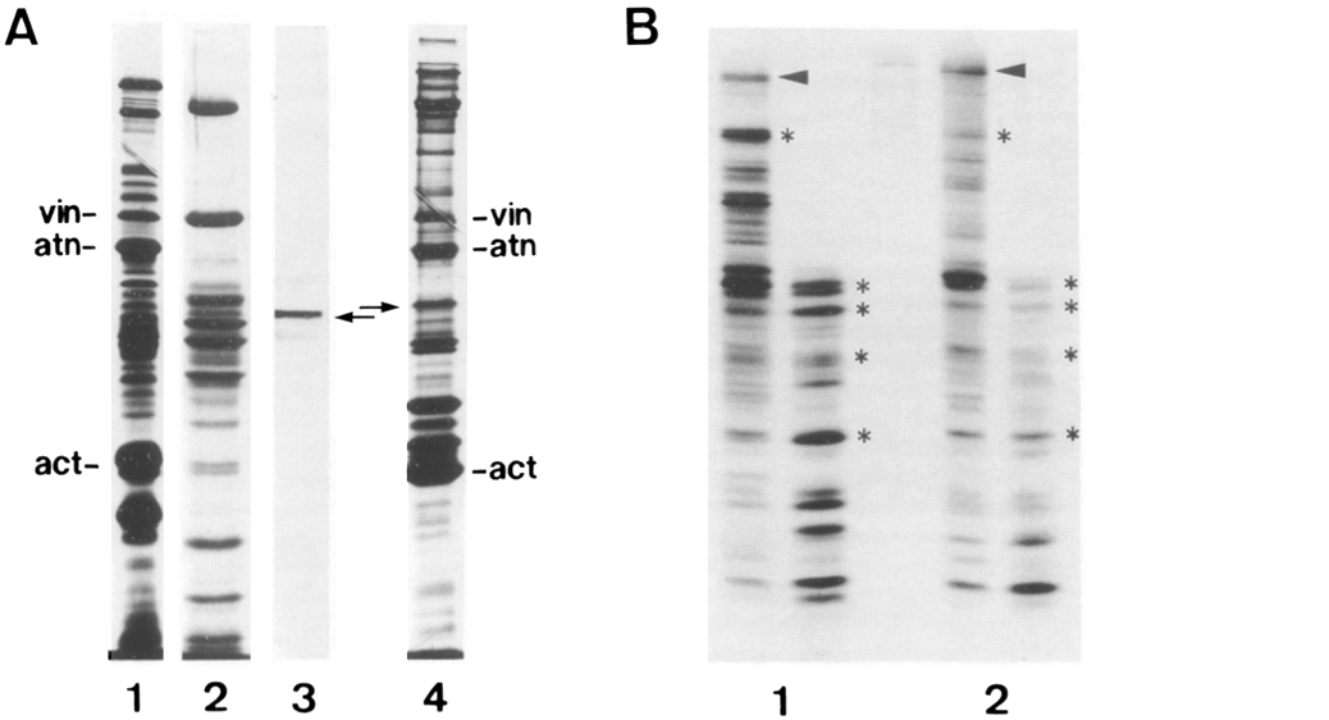

Figure 1. Purification and identification of chicken gizzard radixin. (*A*) SDS-polyacrylamide gels showing the protein profiles during the purification of radixin from chicken gizzard. (Lane *1*) Crude extract of chicken gizzard. Vinculin (*vin*), α-actinin (*atn*), and actin (*act*) are major components of this extract. (Lane *2*) DEAE-cellulose column eluate (60 mM KCl). (Lane *3*) Chicken gizzard radixin eluted from DNase I-actin affinity column. (Lane *4*) Low ionic strength extract of the isolated AJ from rat liver (see reference 38). Note that chicken radixin (*arrow* in lane *3*) has an apparent molecular mass slightly smaller than that of rat liver radixin (*arrow* in lane *4*). (*B*) One-dimensional peptide maps of chicken gizzard radixin (lanes *1*) and rat liver radixin (lanes *2*). The amounts of *Staphylococcus aureus* V8 protease used were 0.1 and 1.0 ng in left and right columns, respectively. Both mapping patterns (*) are similar to each other. *Arrowheads*, nondegraded radixin.

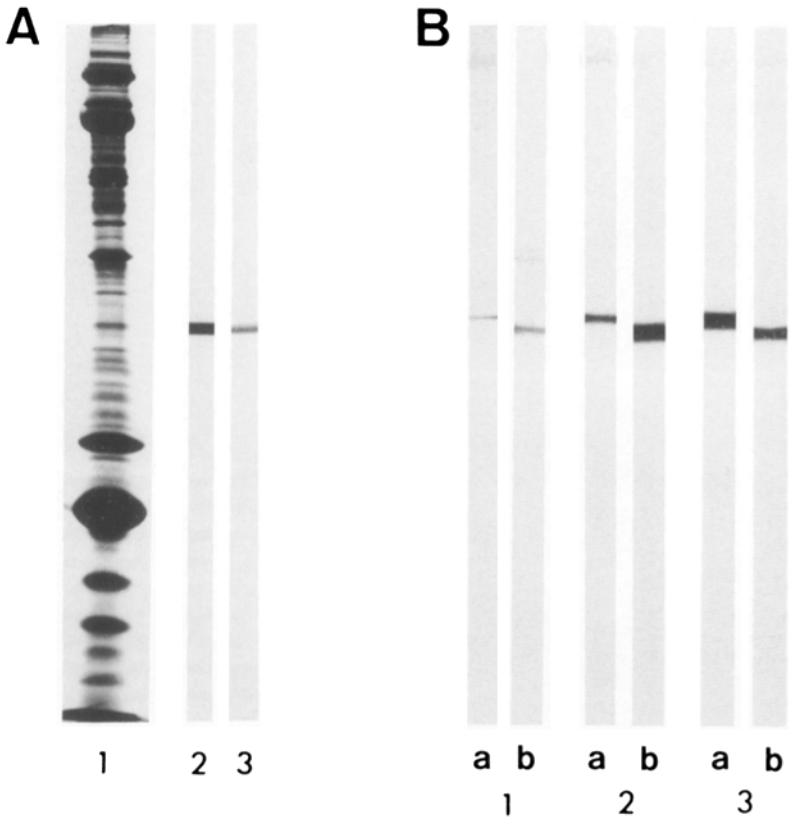

Figure 2. Specificity of anti-radixin mAb and pAb. (*A*) Coomassie blue–stained gel of homogenized chicken gizzard (lane *1*) and accompanying immunoblots by anti-radixin mAb (lane *2*) and pAb (lane *3*). A single band with a molecular mass of ~80 kD (chicken radixin) is specifically recognized by both antibodies. (*B*) Coomassie blue–stained gels (lane *1*) of purified rat liver radixin (*a*) and chicken gizzard radixin (*b*), and accompanying immunoblots using anti-radixin mAb (lane *2*) and pAb (lane *3*).

0.1 mM DTT [pH 7.5]). The crude extract was applied onto the DEAE-cellulose column, washed thoroughly with solution B and eluted with solution B containing 60 mM KCl. The eluate was diluted with an equal volume of solution C (2 mM Hepes, 0.2 mM ATP, 0.2 mM DTT, 1 mM TAME, 1 mM PMSF, 1 μg/ml leupeptin [pH 7.5]). This sample was loaded on the DNase I-actin column (0.8 × 1.5 cm). This column was prepared by mixing gel-filtered G-actin (5 mg) with DNase I-coupled Affi-Gel 10 (see reference 38), followed by thoroughly washing with solution D (mixture of equal volumes of solution B and solution C), solution D containing 400 mM KCl, and solution D, sequentially. After applying the sample, the DNase-actin affinity column was washed with solution D and then radixin was eluted from the column with solution D containing 160 mM KCl. Approximately 3–5 μg of radixin was obtained from 30 g of chicken gizzard.

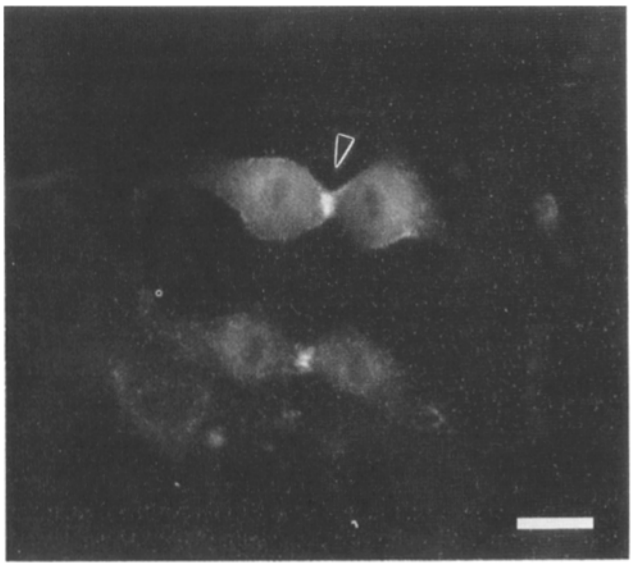

Figure 3. Indirect immunofluorescence images with anti-radixin polyclonal antibody of cultured rat fibroblasts (3Y1 cells). The cleavage furrow of dividing cells (*arrowheads*) appears to be specifically stained, whereas no staining was detected in 3Y1 cells during interphase. Bar, 20 μm. ×500.

Gel Electrophoresis, One-Dimensional Peptide Mapping, and Immunoblotting

SDS-PAGE was based on the discontinuous Tris-glycine system of Laemmli (20). Gels were stained with Coomasie brilliant blue R-250.

For one-dimensional peptide mapping, protein bands to be examined were cut out from the gel, and proteins were eluted electrophoretically. The eluted protein was precipitated by adding 10 vol of acetone, and the pellet was resuspended in water. This sample was subjected to limited proteolysis with *Staphylococcus aureus* V8 protease according to the method developed by Cleveland et al. (6), and electrophoresed in 15% SDS polyacrylamide gels.

For immunoblotting, the samples were electroblotted onto nitrocellulose membranes after SDS-PAGE (42). The strips of the nitrocellulose membranes were incubated with the first antibody and then treated with the second horseradish peroxidase–labeled antibody (Bio-Rad Laboratories, Richmond, CA). The peroxidase was detected by the reaction using diaminobenzidine in the presence of Ni and Co ions (8).

mAb Production

The crude extract from chicken gizzard smooth muscle cells was applied to a DEAE-cellulose column equilibrated with solution B, and eluted with solution B containing 60 mM KCl. After SDS-PAGE, the radixin band was removed with a razor blade, and radixin was electrophoretically eluted from the gel. The eluted protein was precipitated by adding acetone, and the pellet was resuspended in distilled water. This solution was used as the immunogen at each injection.

mAbs were obtained essentially according to the procedure of Köhler et al. (19). BALB/c mice were immunized intraperitoneally with the above immunogen with (days 1 and 14) or without (day 28) CFA. 3 d after the final

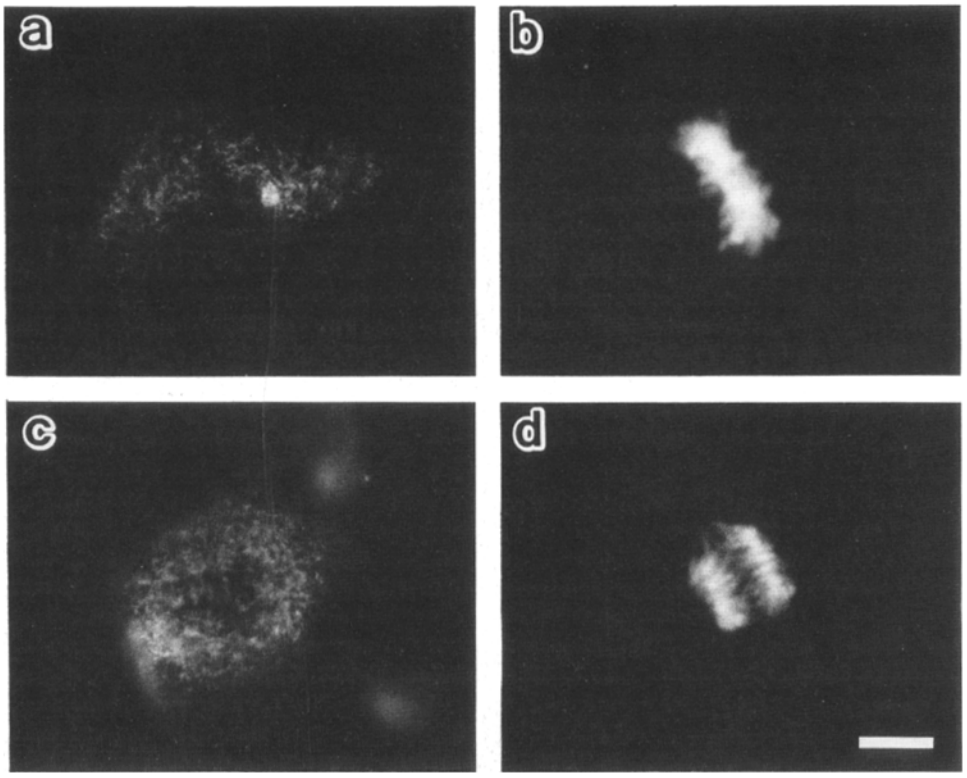

Figure 4. Immunofluorescence staining with anti-radixin mAb in cultured rat fibroblasts (3Y1 cells) at metaphase (*a*) and anaphase (*c*). The chromosome organization of each cell is revealed by staining with DAPI (*b* and *d*). In these rounded-up cells, the characteristic staining on the cell surface increased in intensity as the separation of chromosomes proceeded. Bar, 12 μm. ×800.

injection, the spleens were removed and the splenocytes were fused with mouse P3 myeloma cells. 50% polyethylene glycol (PEG 4000; Merck, Darmstadt, FRG) in RPMI-1640 was used as the fusogen. The initial fusion products were plated in four 24-well plates in hypoxanthine/aminopterin/thymidine (HAT) medium. 6 d after fusion, fusion plates were screened for antibody production with an ELISA assay. The crude extract was used for ELISA assay.

The wells that showed positive activity were immediately expanded and then plated out at clonal density (1.2 cell/well) in a 96-well dish together with feeder cells (thymus lymphocytes). One week after cloning, wells with single clones were tested for antibody with a screening of the immunoblotting analysis using the crude extract. The clones that produced antibodies specifically recognized the chicken radixin were expanded and cloned again.

The antibody-rich supernatant or ascites was used for immunoblotting and immunofluorescence microscopy. Selected clones were grown in mass culture and injected intraperitoneally into pristane-primed mice to produce ascites culture.

Cell Culture

Rat 3Y1 cells were maintained in DMEM supplemented with 10% FBS. For partial synchronization, 3Y1 cells were cultured in DMEM containing 0.5% FBS for 3 d, followed by incubation with DMEM containing 20% FBS. About 1 d after raising the concentration of FBS, many cells began to round up and furrow. Mouse myeloma cells (P3) were cultured in RPMI-1640 containing 10% FBS.

Madin-Darby bovine kidney (MDBK) cells were maintained in Eagle's minimal essential medium containing 0.05 mM Ca^{2+}. Under this low calcium condition, most furrowing cells detached from the substrate, and so were easily collected by gentle centrifugation.

To dissociate the cell-to-cell adherens junctions in MDBK cells, calcium-switch experiments were performed essentially according to Volberg et al. (43). To destroy the junctions, MDBK cells cultured in DMEM were incubated with DMEM containing 3 mM EGTA for 15 min.

Immunofluorescence Microscopy

For indirect immunofluorescence microscopy of cultured cells, the cells on cover glasses were fixed with 1% formaldehyde in PBS for 15 min. The fixed cells were treated with 0.2% Triton X-100 in PBS for 15 min and washed three times with PBS. After being soaked in PBS containing 1% BSA for 10 min, the sample was treated with the first antibody (anti-radixin pAb or mAb, or anti-vinculin pAb [40]) for 1 h in a moist chamber. It was then washed with PBS containing 1% BSA three times, followed by incubation with the second FITC- or rhodamine-labeled antibody for 30 min. For the detection of actin filaments, rhodamine-phalloidin was mixed with the second antibody solution. After incubation, the sample was washed with PBS three times, embedded in 95% glycerol-PBS and examined with a Zeiss Axiophot photomicroscope. In some samples, 4',6-diamidino-2-phenylindole dihydrochloride (DAPI) was mixed in the embedding solution to visualize chromosomes.

Results

Polyclonal and Monoclonal Antibodies Specific for Radixin

As reported previously, we have raised a polyclonal antibody (pAb) specific for rat liver radixin (38). This anti-radixin pAb specifically stains the cell-to-cell adherens junctions not only in rat tissues but also in mouse, bovine, and chicken tissues. However, in some types of cells, the background level of immunofluorescence staining was relatively high in the rounded-up dividing cells. Then, to determine precisely whether radixin accumulates at the cleavage furrow during cytokinesis, we attempted to raise an mAb using rat liver radixin as an antigen. However, probably because the amino acid sequence of radixin may be highly conserved between rat and mouse, we failed to obtain anti-rat radixin mAb. We then tried using chicken radixin as the antigen. Since a preliminary immunoblot analysis showed the occurrence of radixin in chicken gizzard, we first tried to purify radixin from chicken gizzard using immunoblots with anti-radixin

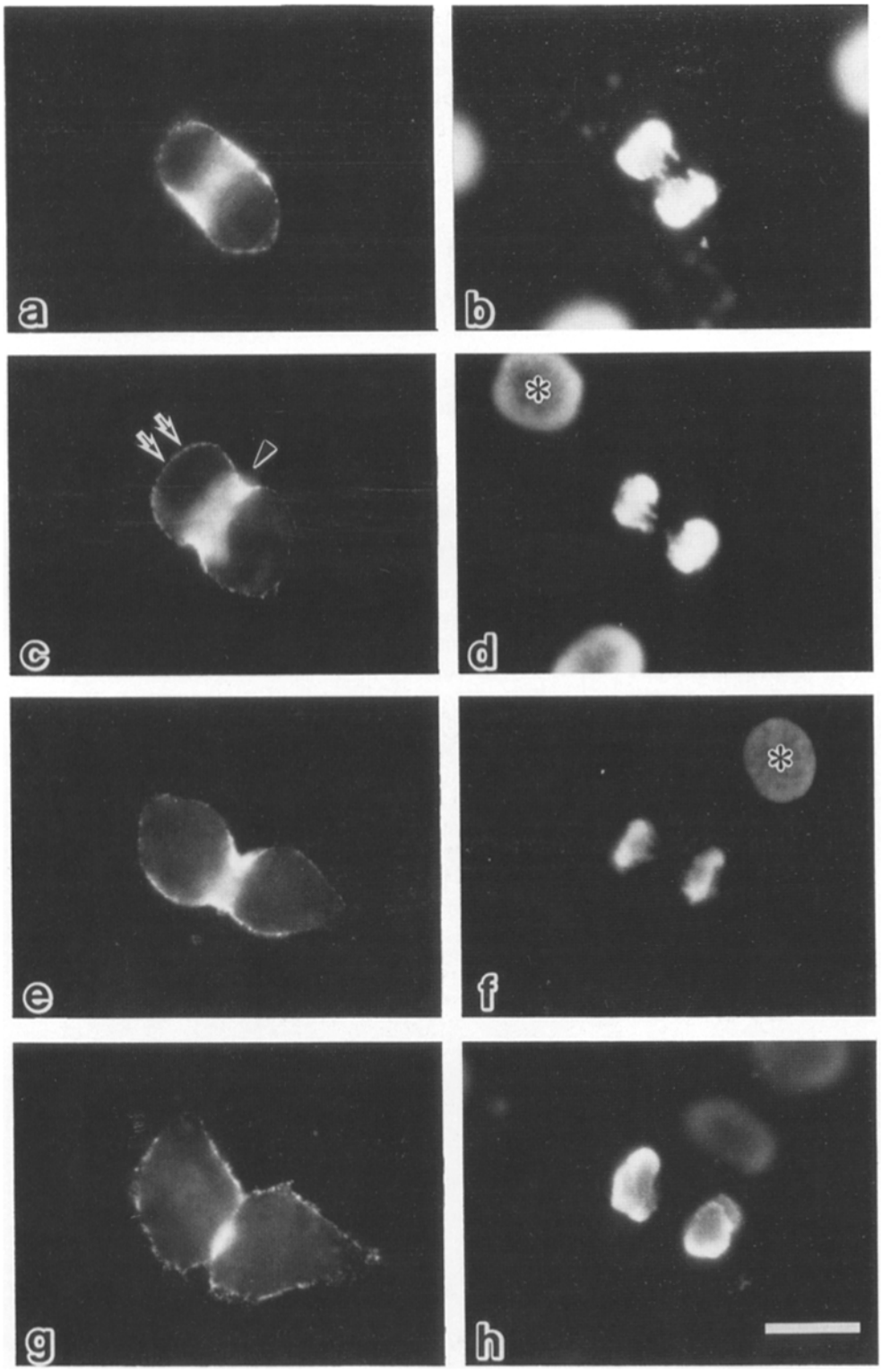

Figure 5. Concentration of radixin at the cleavage furrow of the dividing 3Y1 cells as revealed by anti-radixin mAb (*a*, *c*, *e*, and *g*). The chromosome organization of each cell is revealed by staining with DAPI (*b*, *d*, *f*, and *h*). At the onset of furrowing, radixin appears to be rapidly concentrated at the equatorial cell surface (*a*). Through early telophase (*c*) and midtelophase (*e*), radixin continues to be concentrated at the furrow, and finally distributed at the midbody at late telophase (*g*). Note that at these stages the concentration of radixin at the furrow (*arrowhead* in *c*) is prominent, but the cell surface at the polar region (*arrows* in *c*) is also stained in a dotted manner, not so intensely but clearly. *Nucleus of the cells during interphase. Bar, 20 μm. × 700.

pAb as an assay (Fig. 1 *A*). The chicken radixin was finally purified through its specific binding to an actin-DNase I column. The one-dimensional peptide mapping pattern of this protein was highly similar to that of rat radixin (Fig. 1 *B*). Chicken gizzard radixin has an apparent molecular mass slightly smaller than that of rat liver radixin. Using this chicken radixin as an antigen, we have screened for mAbs that can recognize both chicken gizzard radixin and rat liver radixin. Among mAbs obtained from three mice, only one mAb (called CR-22) was shown to specifically react with radixin both from chicken gizzard and rat liver (Fig. 2). In this study, we have analyzed the concentration of radixin at the cleavage furrow during cytokinesis using our anti-radixin pAb and mAb (CR-22).

Table I. Distribution of 3Y1 Cells Based on Concentration of Actin Filaments and Radixin at the Cleavage Furrow

	High concentration	Moderate concentration	No concentration
	%	%	%
Actin filaments	25	23	52
Radixin	91	9	0

Furrowing 3Y1 cells ($n=122$) at the stage corresponding to Figs. 5, *c* and *e* were analyzed by the use of rhodamine-phalloidin and anti-radixin mAb.

Concentration of Radixin at the Cleavage Furrow during Cytokinesis

Initially, rat 3Y1 cells (fibroblastic cells) were immunofluorescently stained with anti-radixin pAb. As described in a previous paper, no staining was detected in 3Y1 cells during interphase (38). Since 3Y1 cells round up during mitosis, the cells at mitotic phase are easily discerned. Interestingly, these rounded-up cells were intensely stained at their surface, and especially in the dividing cells the cleavage furrow was clearly stained (Fig. 3).

To precisely pursue the dynamic behavior of radixin during a cell cycle, the 3Y1 cells were partially synchronized as described in Materials and Methods, and these cells were doubly stained with anti-radixin mAb (CR-22) and DAPI (Figs. 4 and 5). Judging from the appearance of chromosomes, at metaphase the monoclonal antibody began to stain the surface of rounded-up cells in a characteristic manner as shown in Fig. 4 *a*. As the separation of chromosomes proceeded, the characteristic staining on the cell surface increased in intensity (Fig. 4 *c*). Although the ultrastructural counterpart of this surface staining was not clear, close inspection led us to speculate that some part of this staining might be attributed to microvilli-like structures.

At the onset of furrowing, radixin appeared to be rapidly concentrated at the equatorial cell surface (Fig. 5, *a* and *b*). Through late anaphase and early telophase, radixin continued to be concentrated at the cleavage furrow, and finally distributed at the midbody at late telophase (Fig. 5, *c–h*). In 3Y1 cells, the concentration of radixin at the cleavage furrow was prominent, but the cell surface at the polar region was also stained in a dotted manner, not so intensely but clearly, as shown in Fig. 5.

Next, to compare the distribution of radixin with that of actin filaments during cytokinesis, we have doubly stained the dividing 3Y1 cells with anti-radixin mAb (CR-22) and rhodamine-phalloidin (Table I). As previously reported, the extent of actin concentration in the cleavage furrow appeared to vary considerably among dividing cells. In 3Y1 cells used in this study, only 25% of cells showed a dramatic concentration of actin filaments in the cleavage furrow (Fig. 6), whereas in 52% of cells no actin concentration was detectable in the furrow; 23% of cells showed a moderate extent of concentration. In sharp contrast, anti-radixin mAb and pAb clearly stained the cleavage furrow of all dividing cells. Therefore, in about half of furrowing 3Y1 cells radixin appeared to be concentrated at the cleavage furrow without any significant concentration of actin filaments.

The remarkable concentration of radixin at the cleavage furrow was detected in cells bearing cell-to-cell adherens junctions such as MDBK cells (Fig. 7, *a* and *b*). As previously reported, during interphase the cell-to-cell adherens junction was specifically stained with anti-radixin pAb in this type of cell (38). When the cells went into mitotic phase, these junctions were destroyed, and instead radixin was clearly concentrated at the cleavage furrow. Interestingly, in these cells the cell surface of the polar regions was hardly stained. Cells lacking both cell-to-cell and cell-to-substrate adherens junctions such as myeloma cells also exhibited a

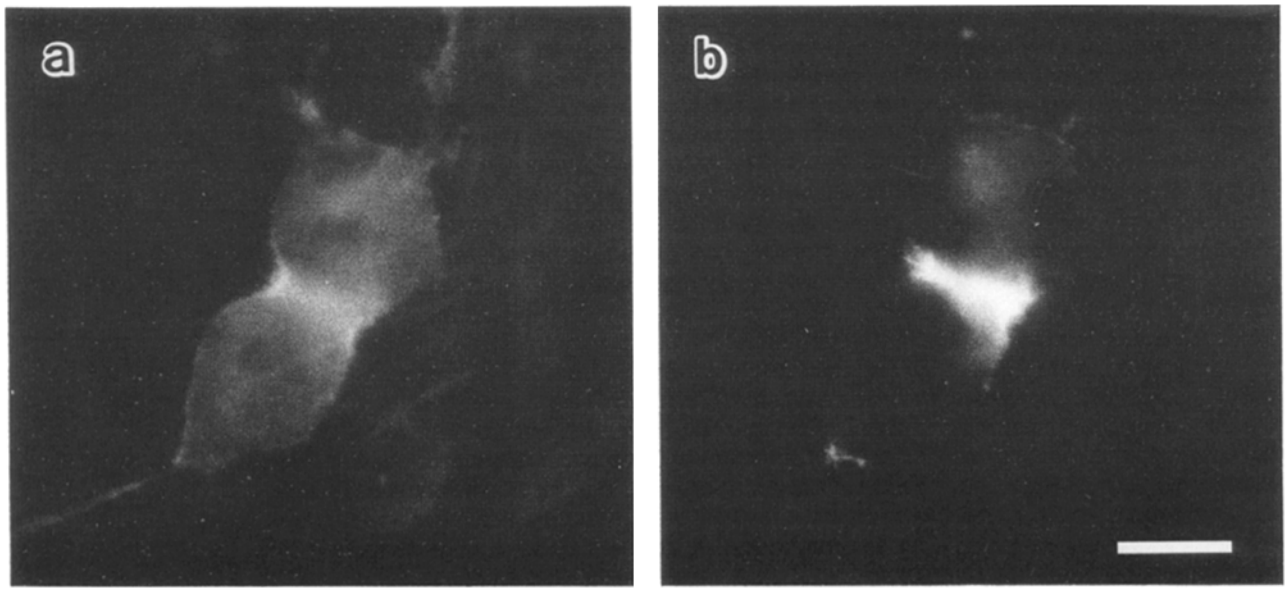

Figure 6. Double immunofluorescence staining with rhodamine-phalloidin (*a*) and anti-radixin mAb (*b*) in a cleaving rat 3Y1 cell in which actin filaments are highly concentrated at the furrow. The shape and size of the radixin-positive band at the furrow are same as those of the actin-positive contractile ring. Rhodamine-phalloidin diffusely stains the cell surface of the polar region, whereas anti-radixin mAb stains it in a dotted manner. Bar, 18 μm. ×1,200.

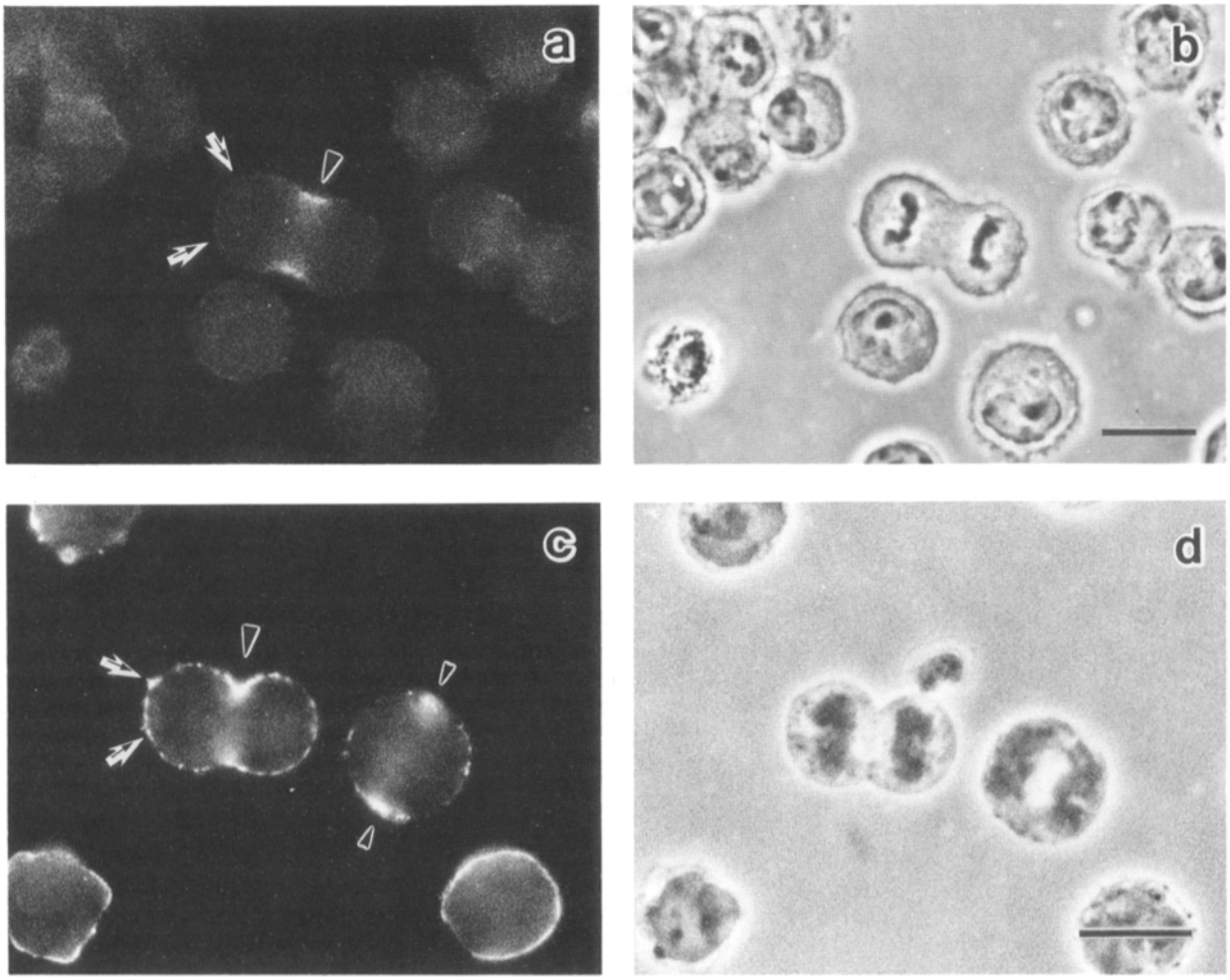

Figure 7. Concentration of radixin at the cleavage furrow in cells bearing cell-to-cell adherens junctions (*a* and *b*) and in cells lacking both cell-to-cell and cell-to-substrate adherens junctions (*c* and *d*). (*a* and *b*) Indirect immunofluorescence image with anti-radixin pAb (*a*) and phase-contrast image (*b*) of MDBK cells. The rounded-up cells were selectively collected as described in Materials and Methods. In this type of cell, radixin shows a clear concentration at the furrow (*arrowhead*), while no staining is detected at the polar region (*arrows*). (*c* and *d*) Indirect immunofluorescence image with anti-radixin mAb (*c*) and phase-contrast image (*b*) of P3 cells. In this case, the equatorial cell surface is clearly stained before furrowing (*arrowheads* in the right cell) and during furrowing the furrow is intensely stained (*arrowhead* in the left cell). In sharp contrast to dividing MDBK cells, the polar region of P3 cells (*arrows*) are also stained. Bars, (*a–d*) 16 μm; (*a* and *b*) ×800; (*c* and *d*) ×900.

clear concentration of radixin at the cleavage furrow, although just like 3Y1 cells radixin occurred also at the cell surface of polar regions (Fig. 7, *c* and *d*).

This concentration of radixin at the furrow was reproducibly observed in all of the various types of vertebrate cells we examined such as rat kangaroo Ptk2 cells, mouse teratocarcinoma cells (F9 cells), and chicken fibroblasts (data not shown). Since neither anti-radixin pAb nor mAb detects a radixin-like protein in sea urchin eggs by immunoblotting analysis (data not shown), we have not been able to analyze the distribution of radixin in dividing sea urchin eggs.

Epitope of Radixin for mAb Is Immunofluorescently Masked in Cell-to-Cell Adherens Junction But Not in Cleavage Furrow

As shown in a previous paper, intense staining is detected in the undercoat of cell-to-cell adherens junctions by anti-radixin pAb (38). However, anti-radixin mAb (CR-22) obtained in this study did not stain the cell-to-cell adherens junctions, whereas the cleavage furrow was clearly stained as shown above. This strongly suggests that the molecular organization of the undercoat differs between cell-to-cell adherens junctions and cleavage furrow, and that the epitope of the radixin molecule recognized by the mAb is masked in cell-to-cell adherens junctions. This interpretation was confirmed in the following experiment using cultured MDBK cells (Fig. 8). The cell-to-cell adherens junctions were not labeled in MDBK cells by CR-22, while they were exclusively stained by anti-vinculin pAb. As reported previously, after extracellular free Ca^{2+} concentration is lowered to the micromolar range, the vinculin-rich junctional undercoat is seen to detach from the plasma membrane (43). Interestingly, this detached undercoat (ring-like structure) was clearly stained by CR-22. These data lead us to conclude that the epitope of radixin for CR-22 is masked in intact junctions, and that this masking is removed by the dissociation of adherens junctions.

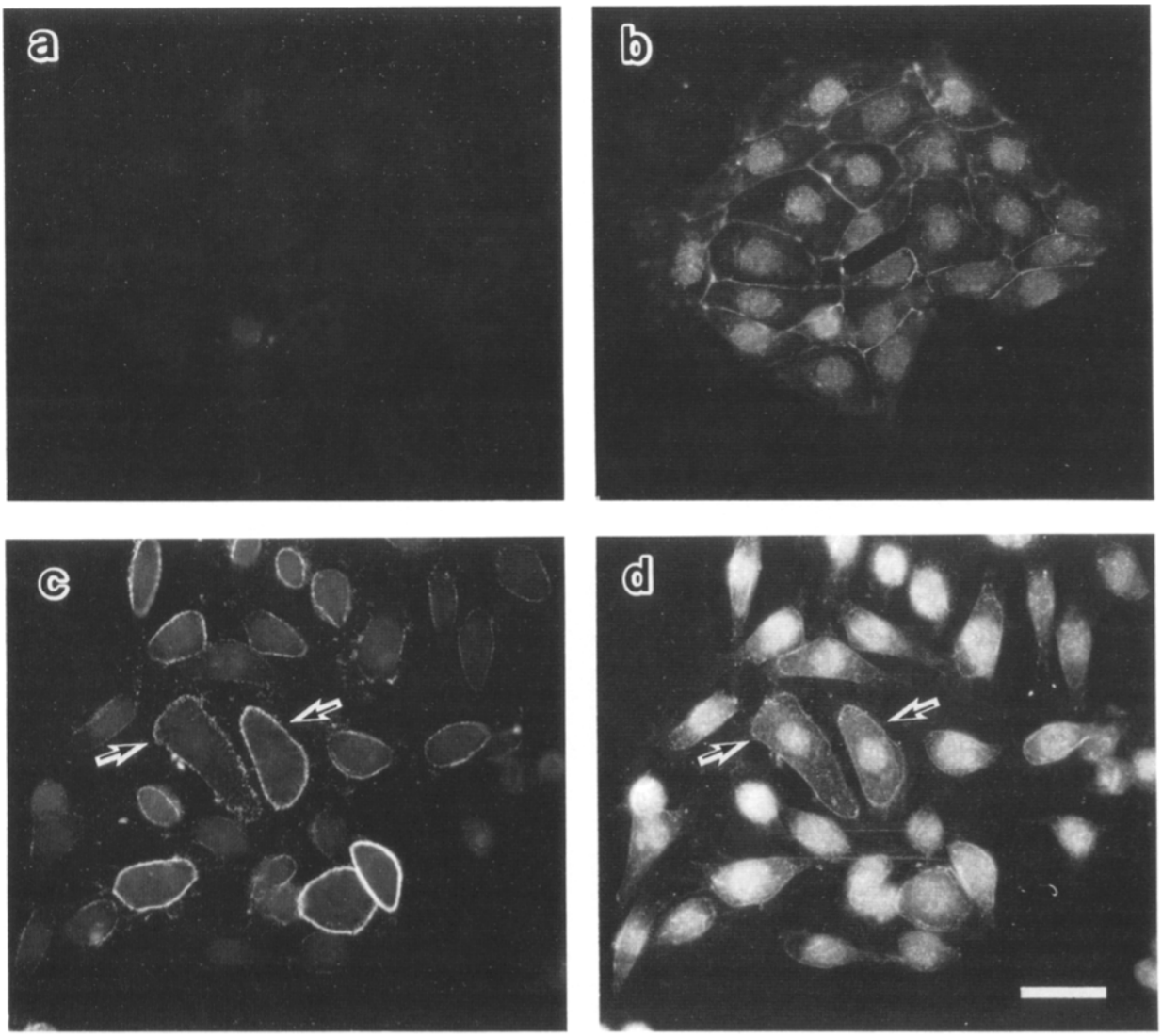

Figure 8. Detection of the epitope for anti-radixin mAb in bovine epithelial cells (MDBK cells) at interphase. Dual-label immunofluorescence images with anti-radixin mAb (*a* and *c*) and anti-vinculin pAb (*b* and *d*). (*a* and *b*) MDBK cells cultured in the medium containing normal concentration of Ca^{2+}. Vinculin can be easily detected at the cell-to-cell adherens junctions, while anti-radixin mAb fails to stain these junctions. (*c* and *d*) MDBK cells 15 min after being exposed to a medium with a low calcium level. The vinculin-rich junctional undercoat appears to detach from the plasma membrane, forming a characteristic ring structure (*arrows* in *d*). Under this condition, this ring structure is clearly stained with anti-radixin mAb (*arrows* in *c*). Bar, 40 μm. ×600.

Discussion

Radixin is a barbed end–capping actin-modulating protein that was first identified in isolated cell-to-cell adherens junctions. In a previous study, we showed that radixin is localized at the undercoat of this type of junction in various types of cells (38). In this study, using anti-radixin pAb and mAb, this protein was shown to be highly concentrated at the cleavage furrow during cytokinesis. The extent of actin concentration at the cleavage furrow has been a subject of hot debate. Some investigators claimed a high degree of concentration (1, 30, 45), whereas others cast doubt on these results (17). In our hands, actin filaments were concentrated in the furrow of only 48% of cleaving 3Y1 cells. In sharp contrast, all cleaving cells showed a concentration of radixin in the furrow. At present, it is not clear whether this discrepancy may be physiologically significant or may reflect problems in preserving actin filaments at the cleavage furrow. However, it may be safe to say that a high degree of concentration of radixin at the furrow indicates an important role for this molecule in the production of cleavage force for cytokinesis.

In spite of intensive morphological and biochemical studies on the contractile ring formed at the furrow, our knowledge of the molecular architecture of this structure is still fragmentary (22, 29, 36). Therefore, it is not easy to guess at the physiological function of radixin, a barbed end–capping protein, at the furrow in situ. Recently, using microinjection of rhodamine–phalloidin or rhodamine-labeled actin, Cao and Wang showed that preexisting actin filaments, probably through movement and reorganization, were used preferentially for the formation of the contractile ring (5). Through electron microscopic analyses of cleavage furrows isolated from newt eggs, Mabuchi et al. also claimed that the actin bundles at the cleavage furrow (cleavage arc) were or-

ganized from preexisting cortical actin filaments (24). Furthermore, they revealed that the preexisting cortical actin filaments were connected to the plasma membrane by granular material at their barbed ends. Together, it is tempting to speculate that this granular material may be the morphological counterpart of radixin molecules, that radixin may bind preexisting cortical actin filaments to the unidentified transmembrane protein, and that this actin-radixin-transmembrane protein complex may move to the furrow during cytokinesis. The occurrence of radixin at the polar regions, though a smaller amount than that at the furrow, appears to favor this speculation (see Fig. 5). Of course, another interpretation would be possible. Further immunoelectron microscopic analyses using isolated cleavage furrows from newt eggs will help to evaluate our speculation.

Through analyses of cells of a mutant of *Tetrahymena*, which lost the ability to furrow during cytokinesis, the expression of an 85-kD protein was shown to be indispensable for cytokinesis (26). Furthermore, immunofluorescence microscopy revealed that in wild-type *Tetrahymena* cells this 85-kD protein was localized at the cleavage furrow during cytokinesis. These data persuaded us to speculate that this 85-kD protein might be *Tetrahymena* radixin. However, our anti-radixin pAb and mAb have never recognized this *Tetrahymena* 85-kD protein, and anti-*Tetrahymena* 85-kD protein antibodies have not reacted with rat liver radixin (data not shown). Since it is possible that rat radixin and *Tetrahymena* radixin are distinct in their antigenicity, the relationship between these proteins will not be clarified until their amino acid sequences are determined.

Our preliminary immunoblot analyses using G_0-, G_1-, S-, and M-arrested 3Y1 cells revealed that radixin appeared to show no remarkable change in its total amount (data not shown). The distribution and expression of radixin at interphase in the cells lacking adherens junctions remain to be clarified in detail using various types of cells. On the other hand, in the cells bearing cell-to-cell adherens junctions, a high degree of concentration of radixin was detected at the cell-to-cell adherens junctions at interphase, and at the cleavage furrow at mitotic phase. Several proteins, including filamin and α-actinin, have so far been reported to be concentrated both in the cleavage furrow and in adherens junctions (1, 11, 22, 23, 29, 32, 36). However, these proteins were also reported to be distributed along actin filament bundles such as stress fibers at interphase. Therefore, among the strictly adherens junction "undercoat-constitutive" proteins (e.g., vinculin [12, 15], talin [2, 3], plakoglobin [7], radixin [38], et cetera), radixin is the first protein to be reported to be concentrated in the furrow of cleaving cells. It is curious that radixin is present in the undercoat of both the cell-to-cell adherens junctions and the cleavage furrow. Of course, it is certain that the molecular architecture of the undercoat of adherens junctions is not identical to that of the furrow; vinculin does not occur at the furrow, and the epitope for our anti-radixin mAb was masked only in the adherens junctions. The most prominent feature shared by adherens junctions and the cleavage furrow is the tight association of actin filaments with plasma membranes. Does radixin play an important role in this association? Studies are now being conducted along this line in our laboratory.

We are particularly grateful to Drs. H. Ohba, Osamu Numata, and Yoshio Watanabe (Tsukuba University) for their cooperation in the comparison between radixin and the *Tetrahymena* 85-kD protein. Our thanks are also due to Drs. E. Muto and H. Hosoya (The Tokyo Metropolitan Institute of Medical Sciences), Dr. Akira Nagafuchi, Miss Noriko Funayama, Mr. Masahiko Itoh, Dr. Takashi Funatsu (National Institute for Physiological Sciences), and Drs. T. Endo, H. Abe (Chiba University) for their helpful discussions throughout this study.

This study was supported in part by research grants from the Ministry of Education, Science and Culture, Japan (to Sh. Tsukita), and by research grants for cardiovascular diseases from the Ministry of Health and Welfare, Japan (to Sh. Tsukita).

Received for publication 12 October 1990 and in revised form 14 January 1991.

References

1. Aubin, J. E., K. Weber, and M. Osborn. 1979. Analysis of actin and microfilament-associated protein in the mitotic spindle and cleavage furrow of PtK2 cells by immunofluorescence microscopy. *Exp. Cell Res.* 124:93–109.
2. Burridge, K., and L. Connell. 1983. A new protein of adherens plaques and ruffling membranes. *J. Cell Biol.* 97:359–367.
3. Burridge, K., and P. Mangeat. 1984. An interaction between vinculin and talin. *Nature (Lond.).* 308:744–746.
4. Byers, H. R., G. E. White, and K. Fujiwara. 1984. Organization and function of stress fibers in cells in vitro and in situ. *Cell. Muscle Motil.* 5:83–137.
5. Cao, L.-G., and Y.-L. Wang. 1990. Mechanism of the formation of contractile ring in dividing cultured animal cells. I. Recruitment of preexisting actin filaments into the cleavage furrow. *J. Cell Biol.* 110:1089–1095.
6. Cleveland, D. W., S. G. Fischer, M. W Kirschner, and U. K. Laemmli. 1977. Peptide mapping by limited proteolysis in sodium dodecyl sulfate and analysis by gel electrophoresis. *J. Biol. Chem.* 252:1102–1106.
7. Cowin, P., H.-P. Kapprell, W. W. Franke, J. Tamkun, and R. O. Hynes. 1986. Plakoglobin: a protein common to different kinds of intercellular adhering junctions. *Cell.* 46:1063–1073.
8. De Blas, A. L., and H. M. Cherwinski. 1983. Detection of antigens on nitrocellulose paper. Immunoblots with monoclonal antibody. *Anal. Biochem.* 133:214–219.
9. Farquhar, M. G., and G. E. Palade. 1963. Junctional complexes in various epithelia. *J. Cell Biol.* 17:375–409.
10. Feramisco, J. R., and K. Burridge. 1980. A rapid purification of α-actinin, filamin, and 130,000-dalton protein from smooth muscle. *J. Biol. Chem.* 255:1194–1199.
11. Fujiwara, K., M. E. Porter, and T. D. Pollard. 1979. Alpha-actinin localization in the cleavage furrow during cytokinesis. *J. Cell Biol.* 79:268–275.
12. Geiger, B. 1979. A 130k protein from chicken gizzard: its localization at the termini of microfilament bundles in cultured chicken cells. *Cell.* 18: 193–205.
13. Geiger, B. 1983. Membrane-cytoskeletal interaction. *Biochim. Biophys. Acta.* 737:305–341.
14. Geiger, B., Z. Avenur, G. Rinnerthaler, H. Hinssen, and V. J. Small. 1984. Microfilament-organizing centers in areas of cell contact: cytoskeletal interactions during cell attachment and locomotion. *J. Cell Biol.* 99:83s–91s.
15. Geiger, B., K. T. Tokuyasu, A. H. Dutton, and S. J. Singer. 1980. Vinculin, an intracellular protein localized at specialized sites where microfilament bundles terminate at cell membranes. *Proc. Natl. Acad. Sci. USA.* 77:4127–4131.
16. Geiger, B., T. Volk, and T. Volberg. 1985. Molecular heterogeneity of adherens junctions. *J. Cell Biol.* 101:1523–1531.
17. Herman, I. M., and T. D. Pollard. 1979. Comparison of purified anti-actin and fluorescent-heavy meromyosin staining patterns in dividing cells. *J. Cell Biol.* 80:509–520.
18. Ishikawa, H. 1979. Identification and distribution of intracellular filaments. *In* Cell Motility: Molecules and Organization. S. Hatano, H. Ishikawa, and H. Sato, editors. University of Tokyo Press, Tokyo. 417–444.
19. Köhler, G., M. Schreier, H. Hengartner, C. Berek, M. Trucco, L. Forni, T. Staehelin, J. Stocker, and B. Takass. 1980. Hybridoma Techniques. Cold Spring Harbor Laboratory, Cold Spring Harbor, NY. 65 pp.
20. Laemmli, U. K. 1970. Cleavage of structural proteins during the assembly of the head of bacteriophage T4. *Nature (Lond.).* 227:680–685.
21. Lazarides, E., and K. Burridge. 1975. α-actinin: immunofluorescent localization of a muscle structural protein in nonmuscle cells. *Cell.* 6:289–298.
22. Mabuchi, I. 1986. Biochemical aspects of cytokinesis. *Int. Rev. Cytol.* 101:175–213.
23. Mabuchi, I., Y. Hamaguchi, T. Kobayashi, H. Hosoya, Sa. Tsukita, and Sh. Tsukita. 1985. Alpha-actinin from sea urchin eggs: biochemical properties, interaction with actin, and distribution in the cell during fertilization and cleavage. *J. Cell Biol.* 100:375–383.

24. Mabuchi, I., Sh. Tsukita, Sa. Tsukita, and T. Sawai. 1988. Cleavage furrow isolated from newt eggs: concentration, organization of the actin filament, and protein components of the furrow. *Proc. Natl. Acad. Sci. USA.* 85:5966–5970.
25. Nunnally, M., J. M. D'Angelo, and S. W Craig. 1980. Filamin concentration in cleavage furrow and midbody region: frequency of occurrence compared with that of alpha-actinin and myosin. *J. Cell Biol.* 87: 219–226.
26. Ohba, H., I. Ohmori, O. Numata, and Y. Watanabe. 1986. Purification and immunofluorescence localization of the mutant gene product of a Tetrahymena cdaA1 mutant affecting cell division. *J. Biochem. (Tokyo).* 100: 797–808.
27. Perry, M. M., H. A. John, and N. S. T. Thomas. 1971. Actin-like filaments in the cleavage furrow of newt egg. *Exp. Cell Res.* 65:249–253.
28. Pollard, T. D., and R. R. Weihing. 1974. Actin and myosin in cell movement. *CRC Crit. Rev. Biochem.* 2:1–65.
29. Rappaport, R. 1986. Establishment of the mechanism of cytokinesis in animal cells. *Int. Rev. Cytol.* 105:245–281.
30. Sanger, J. W. 1975. Changing patterns of actin localization during cell division. *Proc. Natl. Acad. Sci. USA.* 72:1913–1916.
31. Sanger, J. M., B. Mittal, and J. W. Sanger. 1985. Structure and assembly of microfilament bundles. *In* Cell Motility: Mechanism and Regulation. H. Ishikawa, S. Hatano, and H. Sato, editors. University of Tokyo Press, Tokyo. 461–475.
32. Sanger, J. M., B. Mittal, M. B. Pochapin, and J. W. Sanger. 1987. Stress fiber and cleavage furrow formation in living cells microinjected with fluorescently labeled α-actinin. *Cell Motil. Cytoskeleton.* 7:209–220.
33. Schroeder, T. E. 1970. The contractile ring. I. Fine structure of dividing mammalian (HeLa) cells and the effects of cytochalasin B. *Z. Zellforsch. Mikrosk. Anat.* 109:431–449.
34. Schroeder, T. E. 1972. The contractile ring II. Determining its brief existence, volumetric changes, and vital role in cleaving *Arbacia* eggs. *J. Cell Biol.* 53:419–434.
35. Schroeder, T. E. 1973. Actin in dividing cells: contractile ring filaments bind heavy meromyosin. *Proc. Natl. Acad. Sci. USA.* 70:1688–1692.
36. Schroeder, T. E. 1975. Dynamics of the contractile ring. *In* Molecules and Cell Movement. S. Inoue and R. E. Stephans, editors. Raven Press, New York. 305–334.
37. Staehelin, A. 1974. Structure and function of intercellular junctions. *Int. Rev. Cytol.* 39:191–283.
38. Tsukita, Sa., Y. Hieda, and Sh. Tsukita. 1989. A new 82 kD-barbed end capping protein localized in the cell-to-cell adherens junction: Purification and characterization. *J. Cell Biol.* 108:2369–2382.
39. Tsukita, Sh., M. Itoh, and Sa. Tsukita. 1989. A new 400 kD protein from isolated adherens junctions: its localization at the undercoat of adherens junctions and at microfilament bundles such as stress fibers and circumferential bundles. *J. Cell Biol.* 109:2905–2915.
40. Tsukita, Sh., and Sa. Tsukita. 1989. Isolation of cell-to-cell adherens junctions from rat liver. *J. Cell Biol.* 108:31–41.
41. Tsukita, Sh., Sa. Tsukita, and A. Nagafuchi. 1990. The undercoat of adherens junctions: a key specialized structure in organogenesis and carcinogenesis. *Cell Struct. Function.* 15:7–12.
42. Vassen, R. T. M. J., J. Kreike, and G. S. P. Groot. 1981. Protein transfer to nitrocellulose filters. A simple method for quantitation of single proteins in complex mixtures. *FEBS (Fed. Eur. Biochem. Soc.) Lett.* 124: 193–196.
43. Volberg, T., B. Geiger, J. Kartenbeck, and W. W. Franke. 1986. Changes in membrane-microfilament interaction in intercellular adherens junctions upon removal of extracellular Ca^{2+} ions. *J. Cell Biol.* 102:1832–1842.
44. Wessells, N. K., B. S. Spooner, J. F. Ash, M. O. Bradley, M. A. Luduena, E. L. Tayler, J. T. Wrenn, and K. M. Yamada. 1971. Microfilaments in cellular and developmental processes. Contractile microfilament machinery of many cell types is reversibly inhibited by cytochalasin B. *Science (Wash. DC).* 171:135–143.
45. Wang, Y.-L. 1987. Mobility of filamentous actin in living cytoplasm. *J. Cell Biol.* 105:2811–2816.